Structural Health Monitoring of Reusable Launch System using Endovibrator-Type wireless Sensors

Arnaud Kuakuvi, Corinne Dejous, David Barnoncel, Simon Hemour

Structural Health Monitoring of Reusable Launch System using Endovibrator-Type wireless Sensors

Arnaud kuakuvi[#*], Corinne Dejous[#], David Barnoncel[$1], Simon Hemour [#2]

[#]IMS Laboratory, CNRS UMR 5218, Bordeaux INP, University of Bordeaux, France
[$]ArianeGroup SAS, France
[*]now with Freescale semiconductor, France
{simon.hemour}@u-bordeaux.fr

***Abstract* — Modern developments in aerospace industry are shifting towards lighter launchers and aircraft, where every parts are stringently optimized against weight. Within this new design paradigm, mechanical stresses rule of thumb is to be abandoned in favor of real measurement. This calls for lightweight embedded stress sensing strategies to assess the structural health without compromising it. This paper reports the proof-of-concept of new measurement approach to monitor wireless acoustoelastic tension. An endovibrator-type, batteryless wireless sensor is reported. It harnesses the acoustic resonances properties of a metal bolt, and is associated with a Wireless Power Transmission link at 8MHz. Mechanical tension, emulated through temperature variation have been wirelessly captured through the measurements of acoustic velocity variation and the monitoring of the endovibrator inner resonance frequency. A linear dependency is reported with -0.8 kHz/°C at 8.5MHz.**

***Keywords* — ZeroPower, RFID, WPT, SHM, Aerospace, MAIT, backscatter.**

I. INTRODUCTION

As Aerospace industry is shifting towards lighter aircrafts and reusable launchers, there is a heavy need to monitor the flying structure throughout their lifespan. For instance, reusable launch systems need to be assessed at multiple times before liftoff and after the vehicle returns to Earth. Lead time is paramount in such application, and non-destructive structural health assessment is to be done reliably, swiftly, and efficiently.

Among the testing of many elements, the verification of the inter-stage rigidity is critical (red area, Fig. 1). Those interfaces are typically made of bolted junctions. During construction, segments of the launch vehicle are being assembled in horizontal position, using bolts with a determined torque to obtain proper rigidity at the segment junction. In that respect, assessing the bolt tension over the fabrication process is mandatory. Unfortunately, this assessment is obstructed due to accessibility and industrial constraints. In the framework of Ariane 6 development and qualification, over hundreds of bolts need to be measured after the Manufacturing, Assembly Integration and Test (MAIT).

Most of the time, tightening force control on a bolt is done using a torque wrench. Unfortunately, this method is not precise enough for demanding applications. This is because of the nonlinear frictions between various parts of bolted joints [1-3]. For more accurate bolt tightening measurements, such as the one performed in the aerospace industry, piezoelectric sensors can be wired from the bolt to measure its mechanical tension

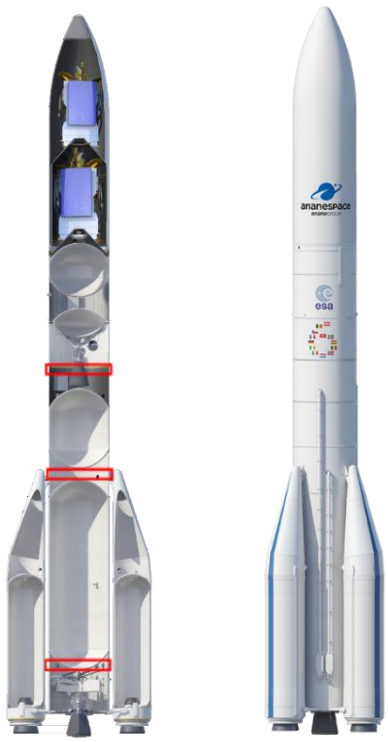

Fig. 1: Schematic of the Ariane 6 rocket. It is composed of individually assembled frames/segments. The red boxes highlight the junctions of about 300 bolts each that are critical for the whole structure integrity. To monitor the structural health of the launch system throughout its construction, pre-launching phase, and post-flight assessment, a significant number of bolts have to be fitted with wireless sensors.

through acoustic properties: Using the ultrasound acoustoelastic method, the time-of-flight of an acoustic wave can be measured across the bolt length, and processed to obtain wave velocity, and eventually extract the longitudinal stress in the material related to the tension [4, 5]. However, such measurements are done in time domain, by connecting a pulse generator and an oscilloscope to the piezoelectric actuator, leading to low signal to noise ratio, and large operational efforts respectively.

This paper proposes a frequency approach derived from the Endovibrator of Leon Theremin [6, 7]. The Endovibrator is an analogue passive device, combining a volume resonator (which

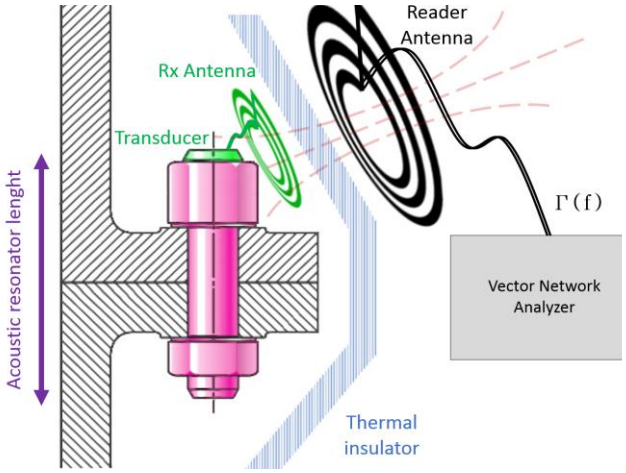

Fig. 2: Tightening torque sensor read-out principle. Wireless power transfer and acoustic resonator are operating at approx. 8HMz

behavior varies depending on a sensing physical parameter) and an antenna (for wireless readout). It has no active devices nor batteries. The Endovibrator technology is infamous for its implementation in a wireless, batteryless microphone, which had been first used to bug the American embassy in Moscow just after WWII [8] (such device remain called “the Thing” in western literature). Impedance modulation is also often seen as the first use of RFID technology [9-11].

This paper first describes the sensing operating principle and the wireless power transfer technique on the ground of which the piezo acoustic endovibrator is developed [12]. Design methodology is then reported. Finally, measurements of the resonance frequency dependence to equivalent tightening torque is demonstrated.

II. Sensing Strategy

The endovibrator-type, wireless bolt tension sensor, is shown in fig 2. The resonator is crafted from the bolt itself glued to a piezoelectric transducer. The metallic bolt is behaving as a very efficient acoustic waveguide. It is terminated with strong acoustic impedance discontinuity, so that standing acoustic wave builds up, with constructive and destructives interferences, yielding in a high resonator acoustic quality factor. When the bolt is being tensioned by the tightening wrench, the acoustic wave velocity is decreasing, impacting thus the resonator effective acoustic length, and its resonance frequency (Fig. 3).

Wireless operation is achieved by implementing a near field Wireless Power Transfer (WPT) link to the piezoelectric transducer.. Impedance matching allows energy to be efficiently exchanged between the inner acoustic resonator and the external reader. As a whole, the endovibrator sensing readout is simply done by reading the resonance frequency from the reflection coefficient (S11) measurements of the one-port system.

The endovibrator key parameter is the quality factor of the inner acoustic resonators because it directly impacts its sensitivity. It is limited by the resonator geometry and losses including the performance of the transducing device. Improvementthe detection limit is often hindered by the

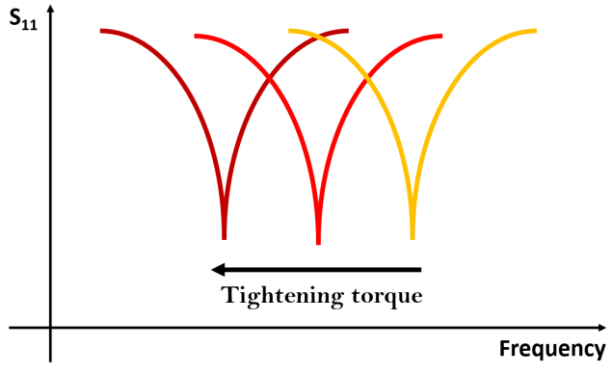

Fig. 3: Sensing operating principle of the acoustic resonator, where frequency of operation is shifting as a function of tightening torque.

available levels of Q-factor, the sensing resolution and the sensitivity related to the spectral shift of resonance in response to variations of the physical property to be measured.

III. Endovibrator Design

A. *Piezoelectric transducer*

Piezoelectric transducer are chosen to operate under the same frequency of operation than the bolt-resonator (about 8 MHz). Its equivalent electrical model is given in fig. 4. It includes the effects of the sensor's mechanical construction and other non-idealities. Key parameters include a series inductance corresponding to the seismic mass and inertia of the sensor itself; and a series capacitance being inversely proportional to the mechanical elasticity of the sensor. The Series resistance correspond to the losses and the power converted into acoustic wave.

The transducer has been chosen from a time of flight perspective: its frequency is well adapted to ultrasound propagation in metallic materials (that is to say high temporal

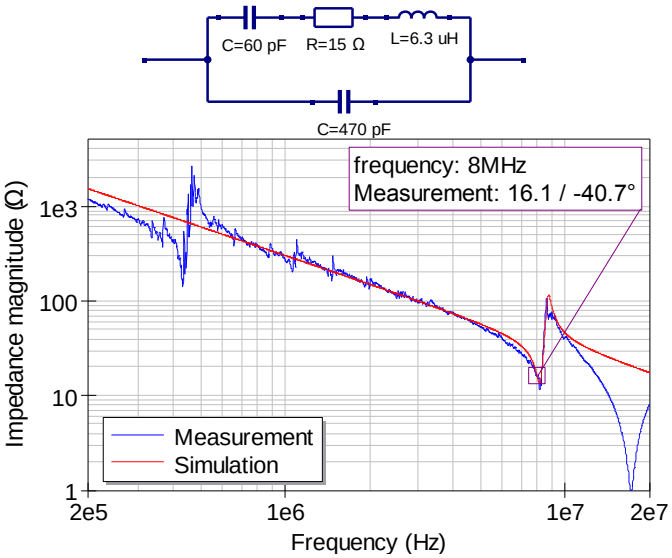

Fig 4: (a) Equivalent model of the piezo sensor, and (b) impedance measurement of piezoelectric transducer before gluing process to the bolt (solid blue line). The simulation of the impedance of the Equivalent piezo model is plotted in solid red line.

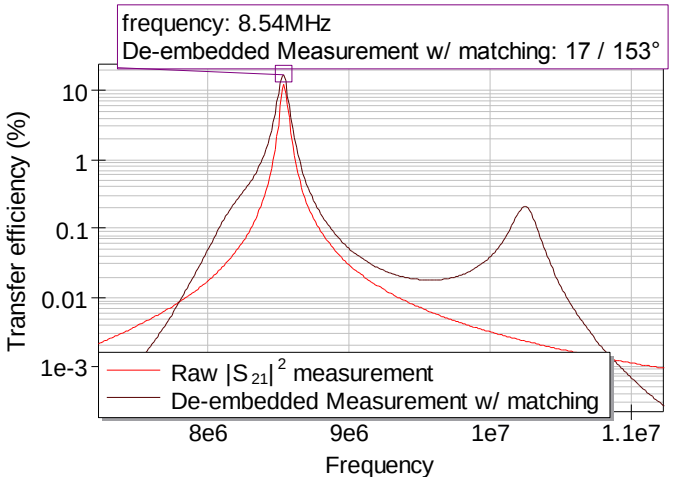

Figure 5: Measurement of the wireless power transfer efficiency of the three-coil resonant magnetic link (red solid line). Expected wireless transfer efficiency between a 50 Ω source and the piezo resistance. The magnetic link is L-matched to the source. A maximum efficiency of 17 % at 8.5MHz is obtained for a distance of 2cm

resolution with low propagation loss). The transducer has been chosen without damping system and with a thickness close to is resonance frequency allowing to use low power signals for generating ultrasound.

B. *Antenna / WPT link*

To carry the power through the load wirelessly, a 3-coils inductive coupling strategy is used (figure 7). The two first coils (excitation + self-resonating) act as the transmitter, while the third as a receiver. The use of 2 coils on the transmitter side allows an isolation between the resistance of the RF source and the self-resonating coil. This yields a better quality-factor, which is key to the power transfer process. A detailed calculation of the S-matrix of a similar system is given in [13]. The third coil powers directly the transducer in this, although a matching network might be necessary.

IV. Measurement Results

A. *WPT Link*

The excitation coil (which can be seen as a reader antenna) is directly powered by the vector network analyzer [14]. It is coupled to the self-resonating coil through a 0.5 cm distance separation, yielding an optimum coupling coefficient the size of the solenoidal coils and their diameters (0.9, 3 and 1.5 cm respectively). The effective WPT distance between the self-resonating (relay) coil and the endovabrator (tag) coil is 2 cm

The raw, three coil resonant link transfer efficiency is plotted in fig. 5 along with the expected *in-situ* performances described in fig. 6. Those are computed by replacing the piezo resistance in the model of fig. 4a by a port. A L-matched circuit is also added to minimize the reflection losses. Note that the series inductor can be integrated with the excitation coil in a future design.

A raw S_{21} gain of -9.2dB is measured from the three coil system. Applying to the measurement data the post-processing described in fig.6, the expected gain becomes -8.7dB, which correspond to a transfer efficiency of 17% from the 50Ω of the

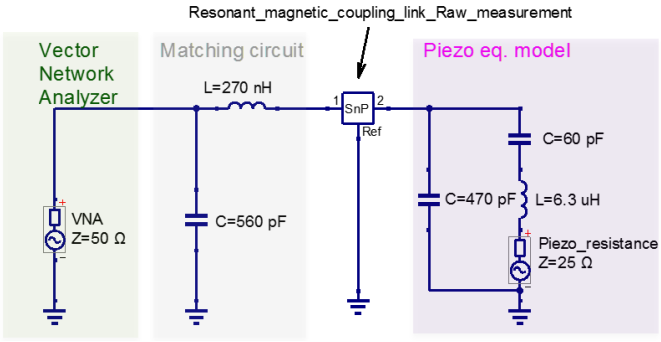

Figure 6: Extraction of the endovibrator wireless readout capability: the resonance magnetic link raw measurement are embedded with the piezo equivalent model, and augmented by a matching circuit. The resistor is replaced by a port, so that transfer efficiency can be computed.

VNA RF source and the active load of the piezo. The transfer efficiency is satisfying enough to ensure that an acoustic wave can eventually be generated within the bolt (forward direction) and then reflected back by the endovibrator through the wireless link (reverse direction). A transfer efficiency that would be too small would hindered result in a reflected electrical wave information that would be buried under the noise floor of the VNA receiver. Next step is to collect the reflection coefficient data from the VNA instrument.

B. *Method*

Scattering matrix [S] parameters are fundamentally mono-harmonics and require the sweeping of continuous-wave measurements over a large frequency span for accurate appreciation of frequency spectrum. Since mechanical resonance have a high quality factor, the intermediate frequency filter bandwidth (IF bandwidth) should be carefully chosen as a tradeoff between frequency resolution bandwidth and the sweep time.

Concerning the transducer under test, it can be considered as a one-port device, connected to the Vector Network Analyzer which allows to collect our targeted parameter: the reflection coefficient. A calibration over the frequency span is performed beforehand to remove the instrumentation and connectivity systematic errors.

Both magnitude and phase of the reflection coefficient are measured by the Vector Network Analyzer corresponding to the time-delayed reflected wave. It is expected that the endovibrator resonance frequency would shift in accordance to

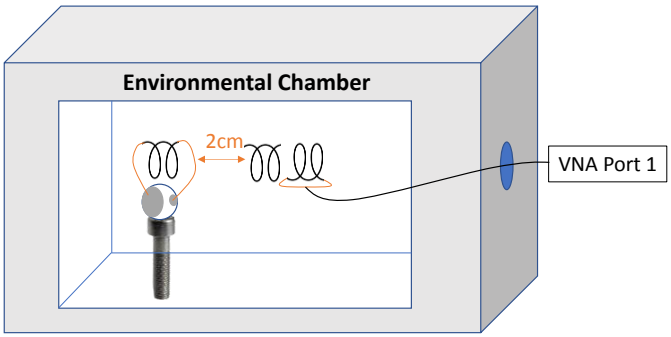

Fig. 7: Measurement setup for the endovibrator. The acoustic phase velocity in the bolt is induced by a change in ambient temperature

the mechanical resonator acoustical dimension and propagation parameter, which are induced by the bolt tightening process and thermal dilatation of the screw. Since a traction force bench is not available for this study, and given that both traction and temperature linearly affect the behavior of the bolt [3], we chose to expose the whole measurement setup to temperature variation thanks to a climatic chamber.

C. Results

The mechanical volume resonator quality factor [15] is first extracted from the measurements of the reflection coefficient in polar plot or in the impedance plane as per the methodology described in [16]. Each of the acoustic cavity resonating modes can be described by a parallel RLC circuit, and correspond to a local loop on the plot (not shown here) where the resonance frequency f_0 is defined as the top of the loop. Two local vectors with an argument of 45° are constructed on the loop to retrieve the 3dB bandwidth $\triangle f$. The acoustic quality factor is calculated as $Q=f_0/\triangle f = 238$ (f_0=8.557MHz and $/\triangle f$=0.036MHz) at 22°C. Note that this value is subject to slight changes depending on the tension or temperature of the bolt.

Since the acoustic resonator is measured through the resonant magnetic coupling link, the three-coil quality factor can also be measured with the same method and yields a Q of 33 (f_0=8.513MHz and $/\triangle f$=0.254 MHz). This value, lower than typical WPT system, is a trade-off between magnetic coupling link efficiency and frequency measurement windows.

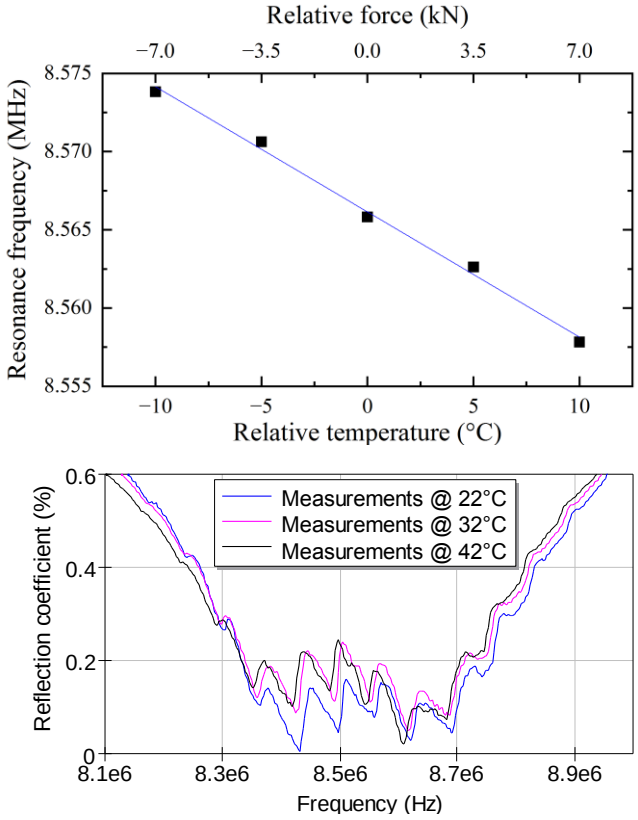

Fig. 8: (a) Calibration curve of the system obtained by from the measurements of the resonance frequency variation versus temperature at 32°C. A coefficient of 698 N/°C is used to convert relative temperature into relative torque. (b) Measurement of reflection coefficient S11 for three temperature conditions.

The screw is placed inside atmosphere and heated by steps of 5 Celsius degrees from 22°C. This relatively large step is chosen at first to ensure notable variations of the different metrics and to overcome the eventual lack of accuracy of the oven. A total of 5 temperatures are then swept at the end of the operation. Measurements are done in both ways, going from lower to higher temperatures and the opposite. This process is repeated through three days to assess the measurement reliability and repeatability.

Results show that the mean shift of each resonance frequency is of -800Hz/°C, which validate the proposed method

ACKNOWLEDGMENT

The authors wish to thank JL. Lachaud and M. Castaings for fruitful discussions.

REFERENCES

[1] T. Wang, B. Tan, G. Lu, B. Liu, and D. Yang, "Bolt Pretightening Force Measurement Based on Strain Distribution of Bolt Head Surface," *Journal of Aerospace Engineering*, vol. 33, no. 4, p. 04020034, 2020.

[2] J. Shao, T. Wang, H. Yin, D. Yang, and Y. Li, "Bolt Looseness Detection Based on Piezoelectric Impedance Frequency Shift," *Applied Sciences*, vol. 6, no. 10, p. 298, 2016.

[3] S. M. Y. Nikravesh and M. Goudarzi, "A Review Paper on Looseness Detection Methods in Bolted Structures," *Latin American Journal of Solids and Structures*, vol. 14, 2017.

[4] Q. Sun, B. Yuan, X. Mu, and W. Sun, "Bolt preload measurement based on the acoustoelastic effect using smart piezoelectric bolt," *Smart Materials and Structures*, vol. 28, no. 5, p. 055005, 2019/04/01 2019.

[5] A. Zagrai *et al.*, *Acousto-elastic measurements and baseline-free assessment of bolted joints using guided waves in space structures* (SPIE Smart Structures and Materials + Nondestructive Evaluation and Health Monitoring). SPIE, 2010.

[6] B. Wwedenski, "Endovibrator (Эндовибратор)," in *Great Soviet Encyclopedia (Большая советская энциклопедия)* vol. 49, ed, 1957, p. 58.

[7] P. Nikitin, "Leon Theremin (Lev Termen)," *IEEE Antennas and Propagation Magazine*, vol. 54, no. 5, pp. 252-257, 2012.

[8] A. Glinsky, *Theremin: ether music and espionage*. University of Illinois Press, 2000.

[9] H. Ribeiro, S. Hemour, and N. B. Carvalho, "Fully Passive Modulation Technique for SWIPT Scenarios," in *2023 IEEE/MTT-S International Microwave Symposium - IMS 2023*, 2023, pp. 999-1002.

[10] K. Gumber, C. Dejous, and S. Hemour, "Harmonic Reflection Amplifier for Widespread Backscatter Internet-of-Things," *IEEE Transactions on Microwave Theory and Techniques*, vol. 69, no. 1, pp. 774-785, 2021.

[11] P. H. Siegel, "Microwaves Are Everywhere: RFID-Do You Know Where Your Pet Is?," *IEEE Journal of Microwaves*, vol. 1, no. 3, pp. 679-688, 2021.

[12] D. Barnoncel and S. Hemour, "Méthode de mesure fréquentielle sans-fil de la tension de serrage d'une vis d'assemblage d'un lanceur spatial," 2022.

[13] A. P. Sample, D. T. Meyer, and J. R. Smith, "Analysis, Experimental Results, and Range Adaptation of Magnetically Coupled Resonators for Wireless Power Transfer," *IEEE Transactions on Industrial Electronics*, vol. 58, no. 2, pp. 544-554, 2011.

[14] S. Hemour and N. Barbot, "Backscattering modulation 101: VNA measurements," in *2023 IEEE 13th International Conference on RFID Technology and Applications (RFID-TA)*, 2023, pp. 169-172.

[15] J.-P. Valentin, "Le coefficient de qualité et ses interpretations," *Bulletin de l'Union des Physiciens,* no. 627, pp. 163-177, Oct 1980.

[16] F. Caspers, "RF engineering basic concepts: the Smith chart," *arXiv preprint arXiv:1201.4068*, 2012.